J Fluoresc (2012) 22:537–548
DOI 10.1007/s10895-011-0991-3

ORIGINAL PAPER

FITC Labeled Silica Nanoparticles as Efficient Cell Tags: Uptake and Photostability Study in Endothelial Cells

Srivani Veeranarayanan · Aby Cheruvathoor Poulose · Sheikh Mohamed · Athulya Aravind · Yutaka Nagaoka · Yasuhiko Yoshida · Toru Maekawa · D. Sakthi Kumar

Received: 11 July 2011 / Accepted: 16 September 2011 / Published online: 29 September 2011

Abstract The use of fluorescent nanomaterials has gained great importance in the field of medical imaging. Many traditional imaging technologies have been reported utilizing dyes in the past. These methods face drawbacks due to non-specific accumulation and photobleaching of dyes. We studied the uptake and internalization of two different sized (30 nm and 100 nm) FITC labeled silica nanoparticles in Human umbilical vein endothelial cell line. These nanomaterials show high biocompatability and are highly photostable inside live cells for increased period of time in comparison to the dye alone. To our knowledge, we report for the first time the use of 30 nm fluorescent silica nanoparticles as efficient endothelial tags along with the well studied 100 nm particles. We also have emphasized the good photostability of these materials in live cells.

Keywords Fluorescent silica nanoparticles · Photobleaching · Photostability · Cell tags · Human umbilical vein endothelial cell · Endothelial cell imaging

Introduction

Real time imaging of live cells helps in understanding the basic biological phenomenon of the organism. Many imaging methodologies use labeled fluorescent dyes or fluorescent microparticles or nanomaterials for imaging normal and pathological pathways of cells or tissues. Traditional systems of imaging use dyes which face many drawbacks such as photobleaching, toxicity, improper biodistribution [1] etc. These drawbacks lead to inefficient live cell imaging due to non-targeted accumulation of dyes and faster rate of photobleaching within minutes. Advancement of nanotechnology has drawn great interest in the area of biological imaging and drug delivery. Nanoscale materials are currently used as fluorescent probes in vitro and in vivo, drug carriers, contrast agents etc., thus aiding in pharmaceutical, therapeutic and diagnostic areas in the medical field [2–6]. Minimized particle size of nanoscale materials is critical for biological intracellular delivery as they are easily taken up by cells. Quantum dots (QDs), dye doped nanoparticles etc., are currently in use for real time imaging of cells. Though QDs are efficient and show less photobleaching compared to fluorescent dyes, most of them are cadmium based and show cytotoxicity and ecotoxicity due to release of heavy metal ions [7, 8]. QDs show less quantum yield than the organic dyes and lead to blinking emission during real time medical imaging. Due to these limitations, fluorescent moiety loaded mesoporous silica nanoparticles can be considered as efficient alternatives for fluorescent dyes and quantum dots. Dye loaded mesoporous nanomaterials possess many unique properties like ordered pores, high surface area, large pore volume and tunable pore size. Due to this tunable pore size and its cargo carrying ability, silica nanomaterials can be considered as efficient reservoirs for biomolecules [9–12]. Recently silica nanomaterials have emerged as excellent drug carriers due to their inertness. They are biocompatible, non-toxic, possess good physicochemical properties and highly accessible for surface modifications [12–14]. Dye doped silica nanomaterials are highly sensitive and are photostable because of protective encapsulation of the silica matrix around the dye molecules [15].

S. Veeranarayanan · A. Cheruvathoor Poulose · S. Mohamed · A. Aravind · Y. Nagaoka · Y. Yoshida · T. Maekawa · D. S. Kumar (✉)
Bio Nano Electronics Research Center Graduate School of Interdisciplinary New Science, Toyo University, Kawagoe, Saitama 350-8585, Japan
e-mail: sakthi@toyo.jp

Silica as fluorescent tags is gaining great importance and many methodologies are employed to synthesize them. Reverse microemulsion and template directed synthesis are usually adopted to synthesize dye doped highly mesoporous nanosilica of size 100–250 nm. Mesoporous silica nanoparticles with CdS gates are utilized as stimuli responsive controlled release agents by Lin et al. [16]. Gadolinium incorporated nano silica synthesized by Lin et al. are used as contrast agents in MRI [17]. Trewyn et al. reported the entry of morphologically different silica nanoparticles into animal cells [18] and the uptake of particles along with their toxicity profile are elaborated by them. These fluorescent nanomaterials are used to track the loaded cargo of drugs in silica nanoparticles in many in vitro and in vivo studies [19–21]. Most of the recent reports emphasize silica nanoparticles of size 100–150 nm as efficient cell labels [22, 23]. However synthesis and utilization of 20–50 nm sized nanosilica as fluorescent cell tags is not well established. Suzuki et al. synthesized 20 nm silica particles which show aggregation and polydispersive nature limiting its application in biological science [24]. Here we report the detailed study regarding the influence of silica particle size (30 nm and 100 nm) on the uptake and internalization by HUVEC cell line and their optical photostability inside live cells. Green color emitting fluorescein dye loaded nanosilica of size 30 nm and 100 nm are successfully synthesized by template directed synthesis and oil in water microemulsion methodology. The cellular uptake efficiency of these two particles is well studied using endothelial cell line- HUVEC. The imminent advantages of the methodology adopted in our work include enhanced biocompatibility and photostability inside live cells of the FITC loaded silica nanoparticles when compared to FITC which is highly detrimental to cell viability. Also, we highlight the increased shelf life of the FITC-Silica nanoparticles, which were found to retain their fluorescence property even after being exposed to light for a period of over one month. Figure 1 provides the schematic representation of the uptake of mesoporous fluorescent nanomaterials by cells via endocytosis.

Experimental Section

Preparation of FITC Precursor Solution

0.5 mg fluorescein isothiocyanate (FITC) was stirred with 1 ml dimethyl formamide (DMF) and 3-aminopropyl triethoxy silane (12 mol% of TEOS) for 2 h under dark at room temperature.

Synthesis of 30 nm FITC Doped Nano Silica

FITC incorporated silica nanoparticles of 30 nm size were prepared by reverse microemulsion method as described herewith: A known amount of cyclohexane and igepal C0-520 were mixed and stirred at room temperature until a clear microemulsion was formed. To the transparent emulsion, 5 ml of tetra ethyl ortho silicate (TEOS) and 1 ml of FITC precursor solution was added and stirred vigorously for 30 min. Later aqueous ammonia was added to catalyse the reaction. The reaction set up was left for stirring at room temperature for 12 h. The resultant product was precipitated with acetone and centrifuged at 10,000 rpm for 10 min to obtain a solid product. This product was repeatedly washed and refluxed in methanolic HCl and desiccated to yield a solvent free 30 nm nano Silica loaded with green fluorescein.

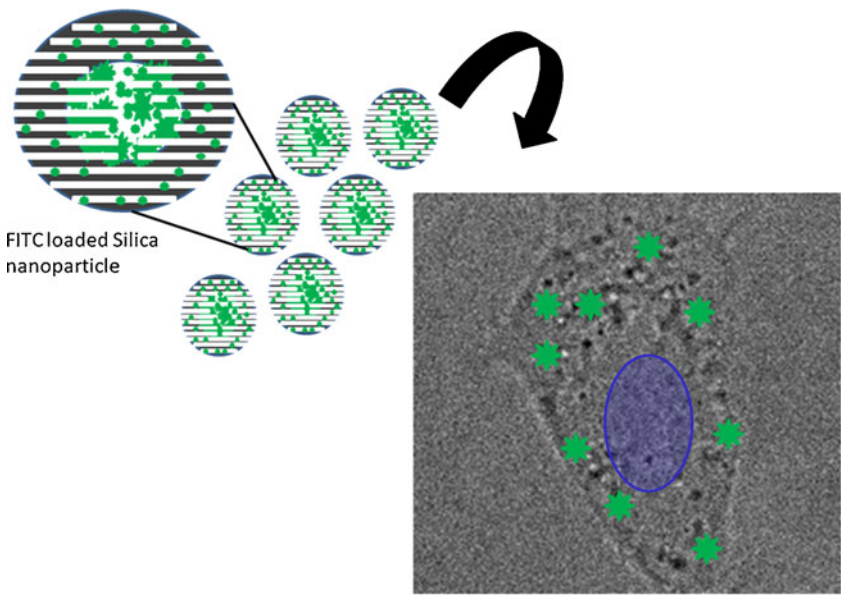

Fig. 1 Schematic representation of cell tagging by using green fluorescein loaded silica nanoparticles

Synthesis of 100 nm FITC Doped Nano Silica

FITC loaded silica nanomaterial of size 100 nm was prepared as per the following method: Silica nanoparticles loaded with FITC were synthesized via modified Stober process by using hexadecyl trimethyl ammonium bromide (CTAB) as template along with TEOS, ammonium hydroxide, ethanol, double distilled water (dd.H_2O). CTAB was first dissolved in dd.H_2O at 75 °C. When the CTAB was completely dissolved, ethanol and ammonium hydroxide were added dropwise sequentially until the pH reaches 10, followed by addition of 5 ml TEOS under vigorous stirring at 80 °C. FITC precursor solution was then added dropwise and the stirring was continued for 8 h at 80 °C. The final orange precipitate was centrifuged at 6,000 rpm for 10 min to obtain the solid filtrate. This was desiccated to remove the moisture, followed by refluxing in methanolic HCl at 70 °C for 24 h to remove the template. The refluxed particles were repeatedly washed with methanol and water and were subsequently desiccated under high vacuum to remove the solvents.

Materials for Biological Studies

Human umbilical endothelial cell lines (HUVEC) were obtained from Gibco. DAPI, Trypan blue, 0.025% Trypsin and XTT tox kit were purchased from Sigma-Aldrich. Alamar blue toxicology kit was purchased from Invitrogen.

Cell Culture Maintenance

HUVEC cells were maintained in T25 flasks using Medium-200 supplemented with Low serum growth supplement and antibiotics (100 U/ml penicillin and streptomycin). The cells were sub-cultured every 2 days. The cells were maintained in glass base dish for confocal studies and plated in 6 well plates for anti-proliferative study and in 96 well plates for cytotoxicity studies.

Particle Characterization Studies

Particle morphology was studied with Field Emission Transmission Electron Micrograph, TEM (JEM-2200-FS). The prepared product was analysed under TEM to obtain fine structure of FITC loaded silica. Multi - BET analysis (Autosorb Quantachrome assisted with AsiQ win software) was carried out to analyze the pore diameter and surface area of the nanomaterials. The UV–vis and PL spectra of plain and FITC loaded silica nanoparticles (30 nm and 100 nm) were studied. The particles were dissolved in dd. H_2O and the UV spectroscopy was carried out using Shimadzu UV-2100PC/3100PC UV visible spectrometer. Photoluminescence spectra were recorded with excitation wavelength 360 nm using Shimadzu F 4500 spectrophotometer. The particle suspension was illuminated using UV and its fluorescence was captured via Pentax Optio W80 digital camera. Dynamic light scattering (Malvern Zetasizer Nano-ZS) was employed to analyze the size of these nanoparticles in dispersion and their dispersive nature was also studied after they were dissolved in dd.H_2O. EDS (JEOL JED-2300T) and XPS (Kratos Analytical) were carried out to analyze the elemental composition of dye doped nano Silica. TGA analysis (Shimadzu DTG-TG 60H apparatus) was carried out using plain silica nanoparticles and dye doped Si nanomaterials (100 nm and 30 nm) and weight loss was plotted against time.

Dye Leaking Studies

The FITC incorporated silica nanoparticles (30 nm and 100 nm) were dissolved in dd.H_2O and sonicated for 3 h and the supernatant was subjected to dye leakage studies under fluorescence microscopy (Nikon Eclipse TE2000-U with Nikon Intensilight C-HGFI).

Photobleaching of Particles

The FITC loaded silica nanoparticles (30 nm and 100 nm) were subjected to continued irradiation using mercury lamp and their fluorescence loss over 2 h has been studied using fluorescence microscopy.

Measuring the Cytotoxicity of FITC Doped Silica in HUVEC

The cytotoxicity of plain silica and FITC loaded 30 nm and 100 nm silica were studied in HUVEC cells using XTT assay and alamar blue assay on 96 well plates. XTT assay utilizes mitochondrial dehydrogenase enzymes of viable cells to reduce the tetrazolium ring of XTT, yielding an orange derivative, which could be identified by absorbance at 450 nm. Alamar blue details about the reduction ability of the cells denoting the active metabolism occurring inside the cell. This active metabolism reduces when the test materials show toxicity leading to reduced reduction capability. The fluorescence intensity of alamar blue assay was quantified at 580–610 nm. 5,000–7,000 HUVEC cells were plated per well and grown for 24 h or until visual confluency was noted. Four different concentrations (1 μg/ml, 100 μg/ml, 500 μg/ml and 1,000 μg/ml) of plain silica, 30 nm and 100 nm doped silica particles dissolved in media were added and incubated for 24 h and assayed further. The experiment was conducted in triplicates and the viability was assessed using a microplate reader (Multidetection

Microplate Scanner, Dainippon Sumitomo Pharma) by measuring the absorbance and fluorescence intensity of the resultant product.

Anti-Proliferative Test

HUVEC cells were plated onto 6 well plates at a count of 50,000–60,000 cells per well. At the time of plating silica nanomaterials (30 nm and 100 nm dye doped silica) were added to the medium and analyzed after 24 h for their anti-proliferative activity.

Fluorescence Phase Contrast and Confocal Microscopy

To visualize the uptake of nanomaterials by the cells, phase contrast fluorescence microscopy and confocal microscopy were employed. Cells were grown on glass base dish for 24 h with standard medium and the fluorescent nano silica of size 30 nm and 100 nm were added separately at a concentration of 100 μg/ml. After 3 h, the nutrient medium was removed and the cells were washed with PBS buffer twice and stained with DAPI and viewed under confocal microscopy (Olympus IX 81 under DU897 mode). The fluorescent intensity loss of nano silica under continued irradiation with green filter in confocal microscopy from 0 h to 1 h was noted. For fluorescence microscopy, cells were grown on 6 well plates as for anti-proliferative test and the fluorescent nanomaterials were added at a concentration of 100 μg/ml on day 2. The cells were incubated for 6 h at 37 °C and washed before viewing under inverted phase contrast microscope with green filter for a period of 1 week.

Flow Cytometry

The cellular uptake of fluorescent nanomaterials has been studied using flow cytometry (JSAN cell sorter, Bay Bioscience). The cells were tagged by fluorescent nano silica and DAPI for nuclear staining. The nano silica was added to the cells on day 2 and the cells are trypsinized as per protocol. The trypisinzed cells were stained with DAPI and subjected to flow cytometry analysis.

Results and Discussion

To prepare green fluorescein doped nano silica, we have utilized two methods: template directed synthesis of porous silica, a modified Stober process and reverse microemulsion technique. As shown in TEM micrographs, the dye doped nano silica showed uniform shape and size with a spherical particle diameter of 30 nm (Fig. 2a) and 100 nm (Fig. 2b). The images also imply that the materials are highly monodisperse without any sign of particle aggregation. The mesoporous pores were clearly visible after removal of template and the so developed structures are well ordered. Nitrogen sorption analysis was carried out to measure the pore diameter of both materials. The pore diameter was 2.07 nm and BET surface area measured was 247.150 m^2/g.

Figure 3 shows absorption spectra of plain and dye loaded silica (FITC-30 nm silica and FITC-100 nm silica) in comparison with pure FITC dissolved in dd.H_2O. Pure FITC showed broad absorption spectrum whereas the dye loaded 30 nm and 100 nm silica showed narrow absorption at around 500 nm. Plain silica showed no absorption. A slight red shift was noted in case of nano silica loaded with dye similar to previous reports [15] when compared to the pure FITC which showed absorption at 480 nm. Figure 4a shows the PL spectra for pure FITC and dye doped nano silica. The excitation wavelength was 365 nm and a clear emission peak was noted around 490–550 nm for all particles. These emission peaks stand typical for green fluorescein FITC. Thus the absorption and PL spectrum complement each other very well depicting successful loading of FITC into nano silica. Figure 4b shows UV illumination of dye doped nano silica of size 30 and 100 nm. The typical green fluorescence was maximum and was captured using digital camera.

Dynamic light scattering (Zetasizer) was utilized to evaluate the size of the dye doped nanomaterials (Fig. 5). The single peak obtained suggests uniform size distribution and monodispersity of the particles. EDS and XPS analysis was performed on FITC incorporated silica nanoparticles. Presence of Si and O and absence of C peak reaffirms that the fluorescein was entrapped inside the silica matrix and was not adhered on the surface of particles (data not shown).

Thermogravimetric analysis were carried out (data not shown). The samples were subjected to 1,000 °C and their weight loss was recorded. Plain silica nanoparticles could withstand upto 1,000 °C with minimal weight loss whereas the FITC doped nanomaterials showed considerable weight loss due to decomposition of FITC when temperature reached 100 °C. Nearly 9% loss of plain silica was noted whereas in 100 nm silica the loss was around 35% and in case of 30 nm silica the loss was around 20%. When the temperature reaches 100 °C (in 10 min) the weight loss was evident in case of loaded nanoparticles which can be attributed to the decomposition of FITC loaded in silica.

Dye leakage from nano silica of size 30 nm and 100 nm (data not shown) was studied by ultrasonicating the nanomaterials in dd.H_2O for 3 h. The sonicated particles were dropped onto glass slides to view dye leakage under fluorescence microscopy using a green filter. There was no evidence of dye leakage even after 3 h of ultrasonication. The particles alone emitted discrete green

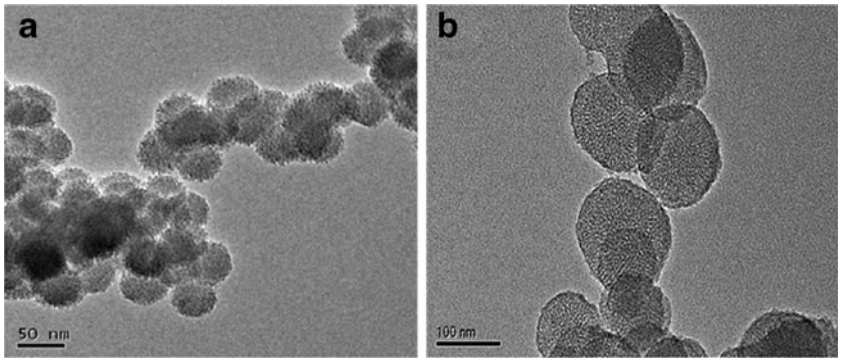

Fig. 2 TEM micrographs of dye loaded porous silica nanoparticles. **a** TEM image of 30 nm dye loaded silica synthesized via microemulsion. **b** TEM image of template directed synthesis of 100 nm dye loaded silica

signals with complete absence of any green fluorescence in the adjacent media suggesting absolutely nil dye leakage from the particles. This shows that FITC gets perfectly functionalized and was completely trapped and guarded by silica matrix.

Photostability measurement of the free FITC and two dye loaded nano silica were noted by fluorescence microscopy. The particles in dry state, as such were added onto petriplates and subjected to continued irradiation using a mercury lamp for 2 h (Parameters used for the study: Lamp—HG precentered fiber illuminator, Nikon Intensilight mercury lamp, with GFP-B filter of excitation 460–500 nm and barrier 510–560 nm, 20X magnification. The distance between lamp and lens was 20 cm, lens and condenser was 8 cm and condenser and sample was 6 cm). Images were acquired at 60 min intervals. The fluorescence intensity of the region of interest was measured. We observed 100% loss of fluorescence in FITC within 30 min (Fig. 6a) and 78% and 92% retention of fluorescence in 30 nm and 100 nm particles respectively. However after a period of 2 h, we noted 57% and 70% of fluorescence intensity retention in 30 nm particles (Fig. 6b) and 100 nm particles (Fig. 6c) respectively. This clearly shows us that encapsulating or efficient loading of dye into nanomaterials can substantially increase the photostability of the dye leading to enhanced fluorescence and long time stability of fluorescence, which can be used for imaging purpose. The improved photostability of the FITC-silica nanoparticles was greatly complemented by the fact that they exhibited considerable fluorescence even after a month under continued irradiation of normal light, highlighting their durability and extended shelf life.

Cytotoxicity profile of plain FITC, plain nano silica and dye doped nano silica of size 30 nm and 100 nm were studied on HUVEC cells using XTT and Alamar blue assay grown on 96 well plates. The nanomaterials were added to the cells. We observed that cell viability decreased as a function of concentration and time. The densities of viable cells are reported in Fig. 7a (XTT) and b (Alamar blue assay) observed under different concentrations after 24 h incubation with the nanomaterials. The cells showed uptake of nanomaterials within 3 h of incubation as evidenced from confocal studies and hence it is concluded that by 24 h the cytotoxic studies can be carried out. Plain FITC showed comparatively higher toxicity even at the lowest concentration. It is clear that the cell viability was higher than 91% even at the highest concentration of 1 mg/ml of FITC loaded silica nanoparticles highlighting the biocompatibility of these nanomaterials. Plain nano silica too showed 95% cell viability at higher concentration denoting complete removal of solvents/templates from the particles. This clearly shows that these nanomaterials exert no significant cytotoxic effects on endothelial cells and thus present themselves as highly safe labeling probes compared to FITC.

HUVEC cells are known for their proliferative activity. They can reach 100% confluency within 48 h after subculture. Their mitotic index is high and they double their count within 2–3 days. This proliferative nature of HUVEC was tested against highest concentration of dye loaded nano Silica (1,000 μg/ml of 100 nm and 30 nm particles). The cells were counted and diluted to a concentration of 2×10^5 cells/plate. The cells were added along with nanomaterials and incubated at normal growth condition. The cells were trypsinized on day 3 and counted

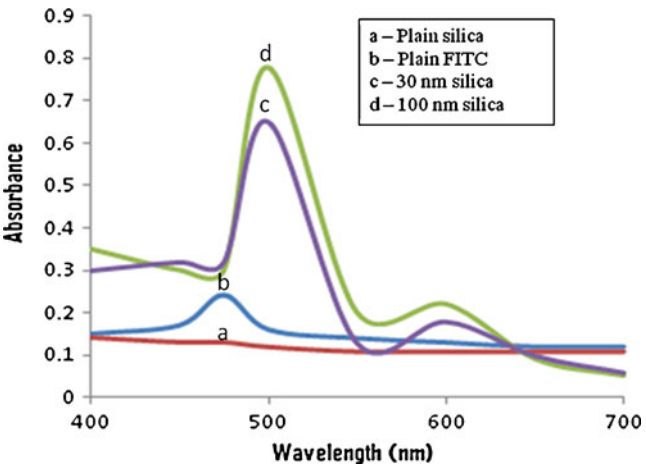

Fig. 3 UV–vis absorption spectra of pure FITC, plain silica and fluorescent nanomaterials

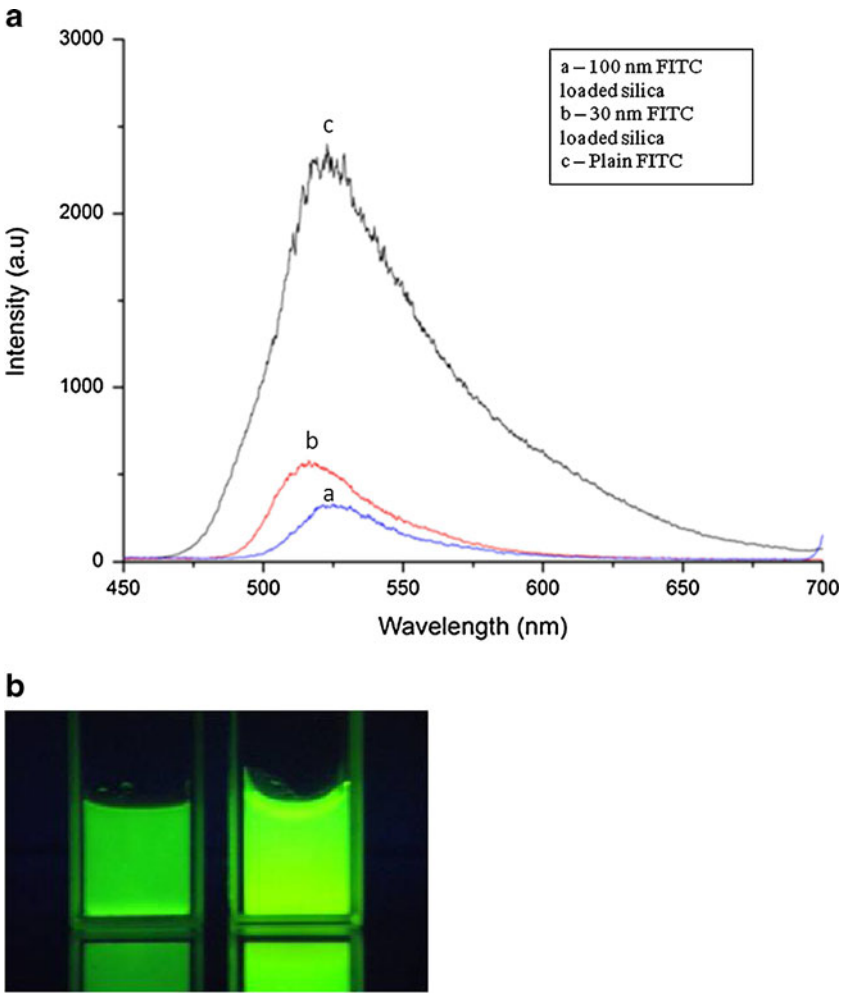

Fig. 4 Photoluminescence characterization. **a** Photoluminescence spectra of the fluorescent nanomaterials compared with pure FITC. **b** UV illumination of fluorescent silica nanomaterials. Left: 30 nm fluorescent nanomaterials and Right: 100 nm fluorescent nanomaterials

using trypan blue in a Countess automated cell counter, Invitrogen. The counts showed 5×10^5 cells per well, same as in control plates, which showed that these nanomaterials do not exhibit any anti-proliferative effect on HUVEC cells and they are cyto-amiable. Nearly 98% cells are found to be viable and excluded trypan blue, citing nil toxicity and anti proliferative effect. These observations thrust the inevitable fact that these nanomaterials can be effectively used for in vivo vascular lineage tagging without any side effects whatsoever.

Cellular uptake and endocytosis of these nanomaterials were studied by confocal and fluorescence microscopy to determine the intracellular fate of these nanomaterials. Cells were treated with as low as 100 μg/ml of nanomaterials and incubated for 3 h. After 3 h, the cells were viewed under fluorescence phase contrast microscope excited using mercury lamp. The fluorescent and phase contrast images of the cells are shown in Fig. 8a (30 nm) and 8b (100 nm) which show the time evolution pattern of cells labeled with dye doped nano Silica. The fluorescence was noted as a function of time from day 0 to day 6. The images clearly depict that the fluorescence retained until day 6 but slow photobleaching was observed as time progresses in case of 100 nm particles whereas no fluorescence was observed in 30 nm particles at day 5. The decrease in fluorescence

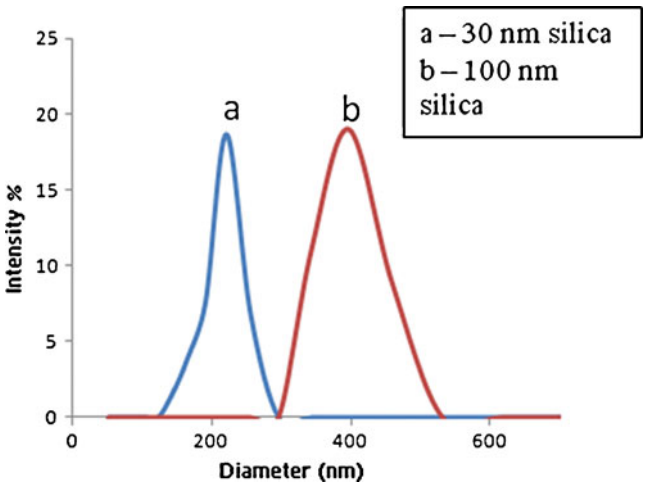

Fig. 5 Particle size analysis of 30 nm and 100 nm silica by DLS. The hydrodynamic diameter of 30 nm particles is 200 nm and of 100 nm particle is 425 nm

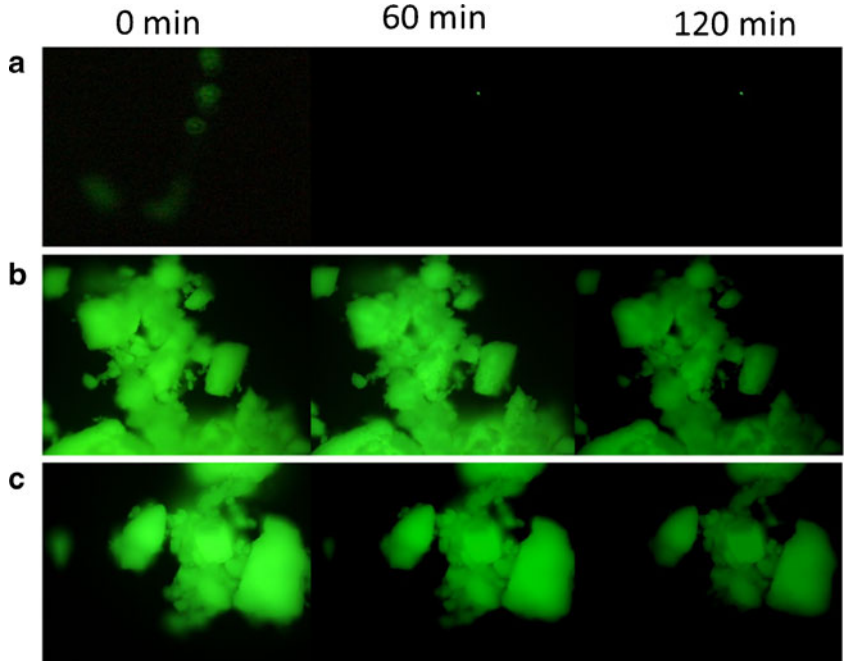

Fig. 6 Time course measurement of photostability. The dry state nanoparticles are subjected to continued irradiation and images are taken every 20 min. Images shown here are taken at 0 min, 60 min and 120 min. **a** Plain FITC. **b** 30 nm fluorescent silica particles. **c** 100 nm fluorescent silica particles

intensity can be attributed to the high mitotic index of HUVEC cells. Because of the high number of mitotic cells, they divide at a rapid rate leading to sharing of nanomaterials from parent cell to the daughter cells, resulting in decreased particle concentration in each cell by 50% on day3 (HUVEC divides once in 3 days) and 25% on day 6. This process dilutes the nanomaterials per cell and leads to reduced fluorescence intensity. Another notable factor for loss of fluorescence can be attributed to the efficient exocytosis of these nanomaterials by HUVEC cells.

To confirm the uptake of particles and viability of cells after nanoparticle entry, confocal microscopy was carried out and the images are shown in Fig. 9a (30 nm) and b (100 nm). The cell's nucleus was stained with DAPI to clearly depict the cell viability. All the cells studied presented perfect DAPI staining of nucleus, proving that they were viable till day 7. The confocal images clearly provide evidence for the presence of nanomaterials in the cell's cytoplasm, crossing the plasma membrane of cells. The discrete green dots showed the nanomaterials were effectively internalized, most likely through endocytosis. The green fluorescence was seen in the cytoplasm, probably entrapped in the vesicles around the nucleus. This suggests that there is no nuclear permeability of nanomaterials. The discrete green dots remain as such localized, reporting no leaching of dye. The time dependent uptake of nanomaterials is presented in Fig. 10a and b at 4 h and 8 h respectively, which shows the uptake increases with time. The fluorescence of these nanomaterials internalized in cells were also observed after a week (day 7, Fig. 11) depicting less photobleaching in case of 100 nm particles, whereas no fluorescence was noted with 30 nm particle on the same day. This clearly proves that FITC is still embedded in silica matrix. However, the discrete dots of fluorescent intensity disappeared, suggesting the spread of fluorescence throughout the cytoplasm, which predicts the escape of nanomaterials from endosomes to cytoplasm. This escape of nanomaterials from endosomal vesicles to

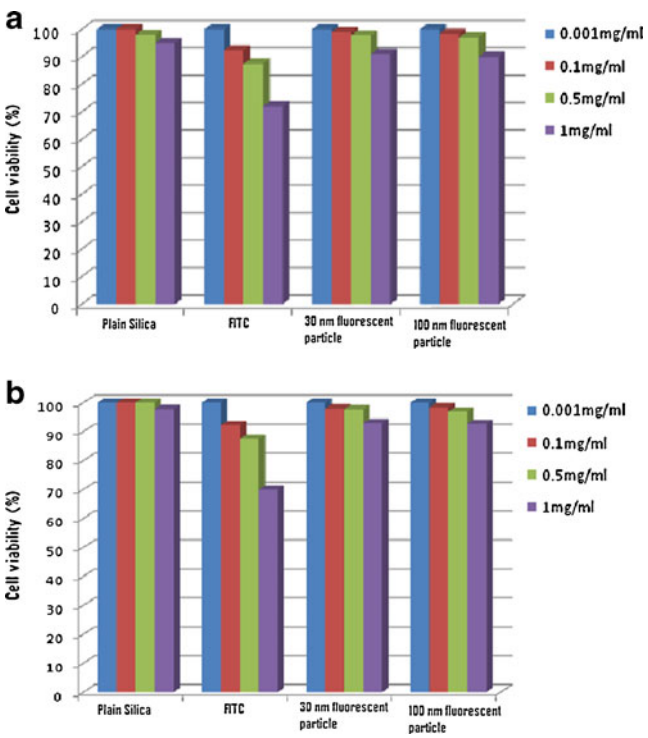

Fig. 7 Cytotoxicity profiling of plain silica nanoparticles, pure FITC, FITC loaded 30 nm and 100 nm silica particles on HUVEC, Endothelial cells. **a** XTT assay and **b** Alamar blue assay

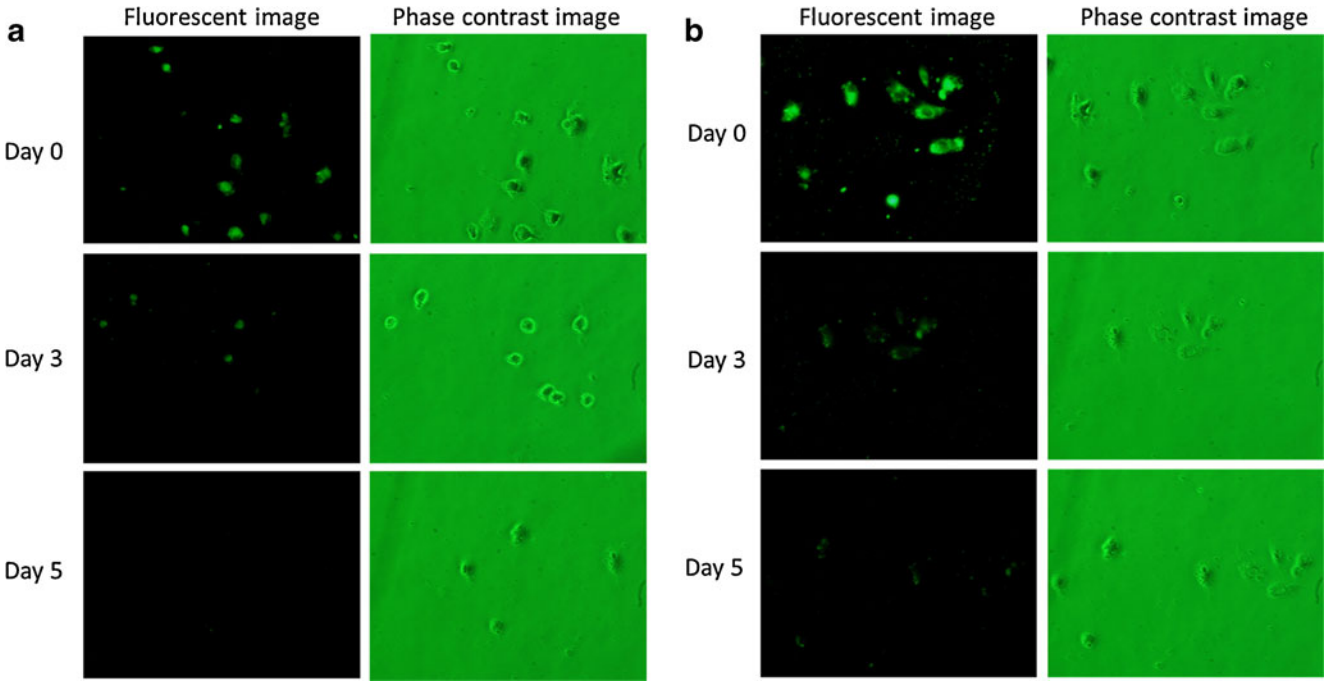

Fig. 8 Phase contrast and fluorescence microscopical images of HUVEC cells tagged with dye doped silica nanoparticles on day0, day3 and day5. **a** 30 nm particle treated cells. **b** 100 nm particle endocytosed cells

cytoplasm evidenced by imaging with the help of FITC loaded silica nanoparticles can stand as an important factor in regard to drug loaded Silica nanomaterials which is an essential aspect in therapeutic treatment. Photobleaching of internalized nanomaterials were studied via continued irradiation using 488 nm excitation. Images recorded every 20 min with fluorescence bleaching for a period of 1 h under continued irradiation are shown in Fig. 12a (FITC alone), 12b (30 nm) and 12c (100 nm). The fluorescence intensity of region of interest was measured at every 20 min and fluorescence loss intensity was plotted verses time which is shown in Fig. 13. In case of plain FITC, the loss was 100% within 20 min. No fluorescence of FITC was noted after 20 min continued irradiation denoting the bleaching of free dye inside live cells. But in the case of 100 nm particles, the fluorescence intensity decreased to 60% under continued irradiation and in case of 30 nm particles was reduced to 52%. After 1 h, the fluorescence intensity of 100 nm particle decreased to 30% and 30 nm particle decreased to 17.2% which shows that fluorescent

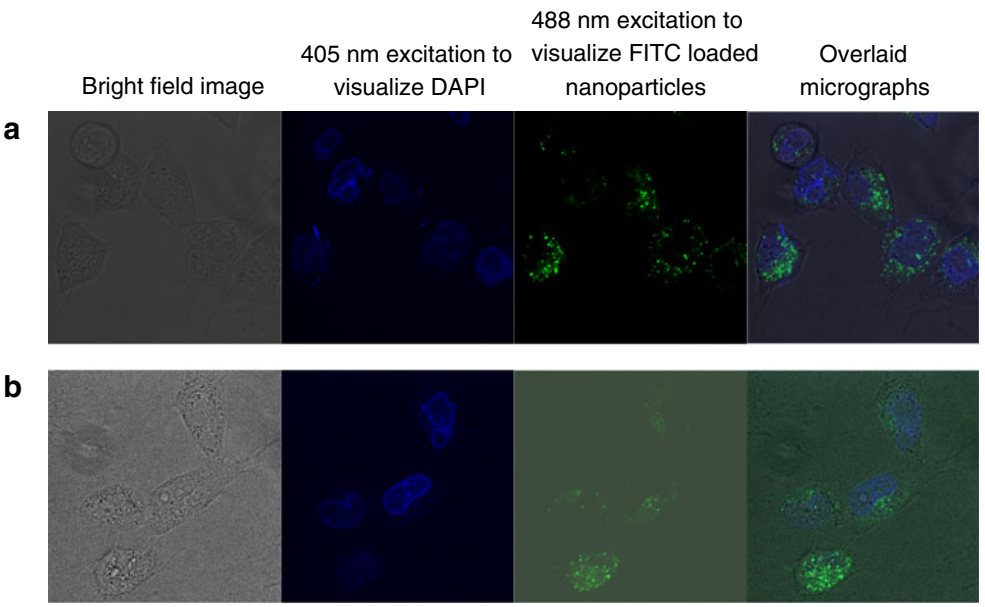

Fig. 9 Confocal micrographs of HUVEC cells with endocytosed 100 μg/ml fluorescent silica nanomaterials. **a** Cells which endocytosed 30 nm particles and **b** 100 nm particles. The cells are incubated with the particles and washed and subjected to confocal microscopy. The green discrete dots shows the internalization of particles into cells and blue DAPI staining proves the viability of HUVEC cells

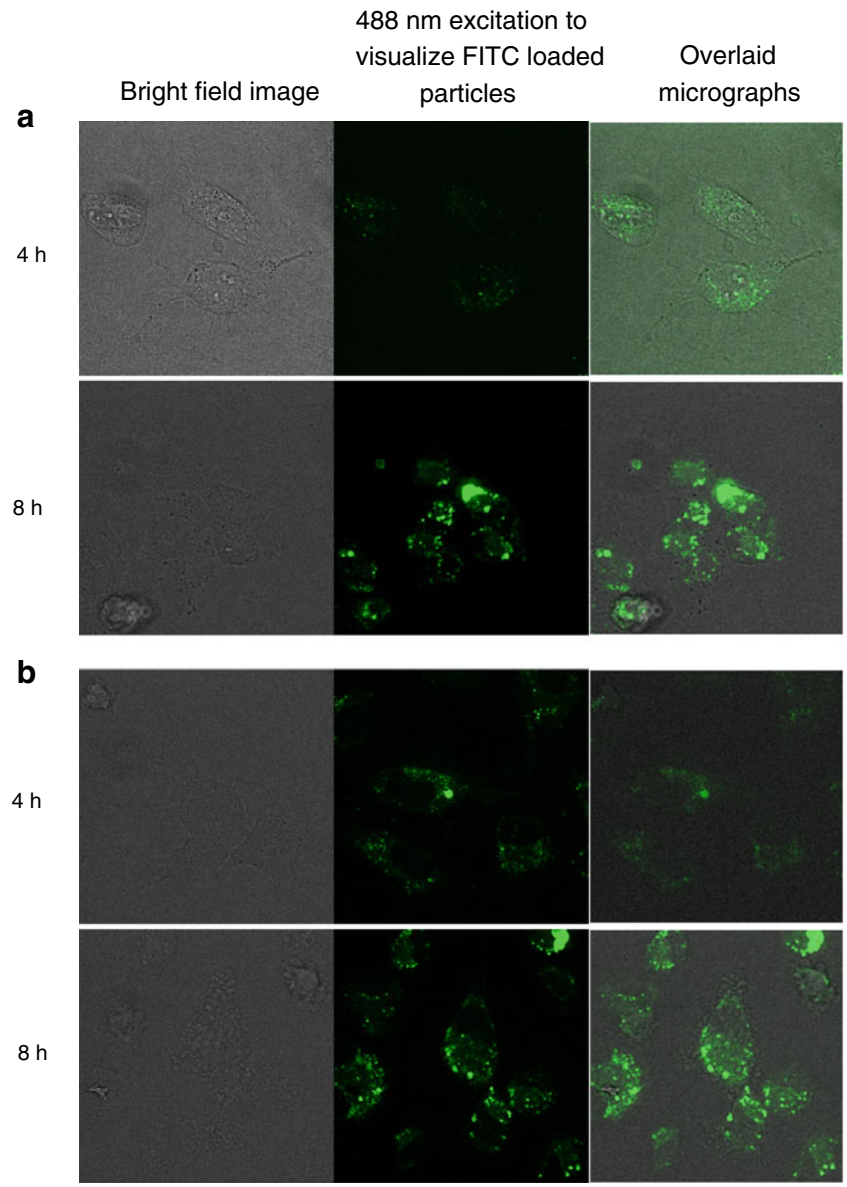

Fig. 10 Time dependent uptake of nanomaterials. **a** 30 nm fluorescent nanoparticle treated for 4 h and 8 h. **b** 100 nm fluorescent nanoparticle treated for 4 h and 8 h. The uptake of nanomaterials are time course dependent and are high at 8 h. The cells are incubated with 100 μg/ml particles for given period of time, washed and then viewed under confocal microscopy

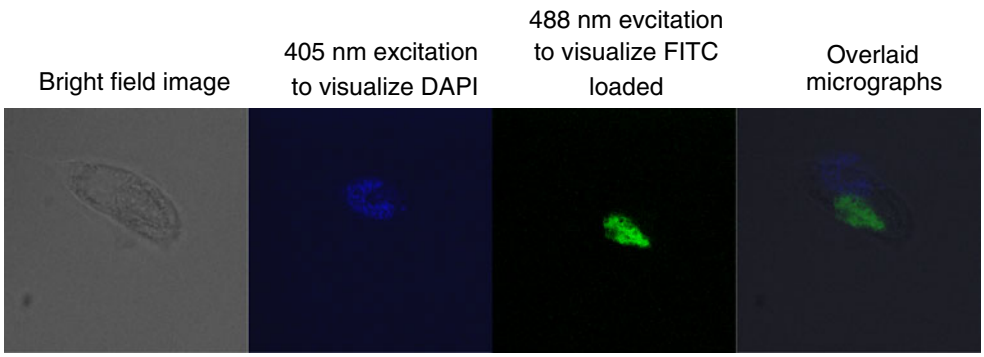

Fig. 11 Confocal micrographs of HUVEC cells showing fluorescence after a week. The particles are added at a concentration of 100 μg/ml and the cells are washed next day. This clearly shows that entrapped particles in the cells shows fluorescence after 1 week. The discrete dot patterns have changed to cytoplasmic fluorescence floods but the fluorescence can be still noted efficiently. This shows enhanced photostability of these nanomaterials

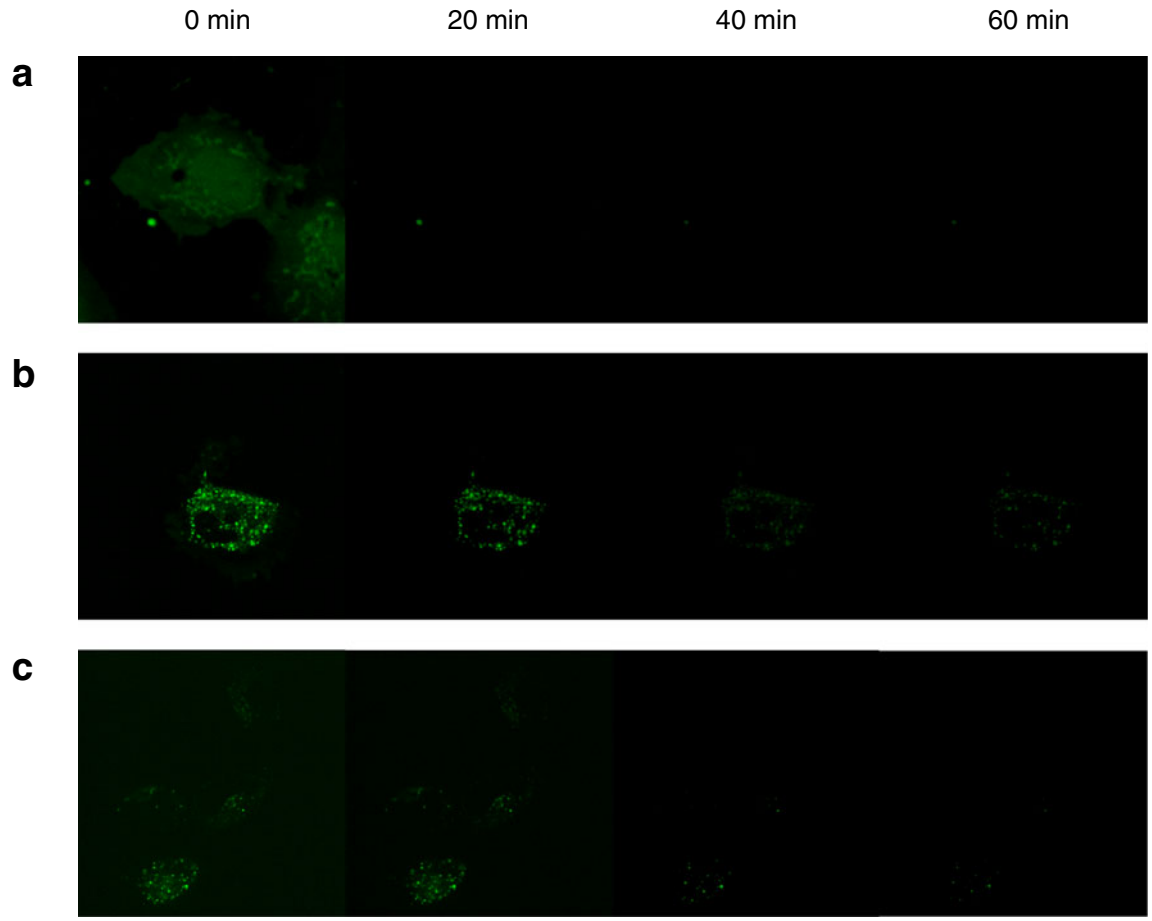

Fig. 12 Confocal micrographs of continued irradiation of cells leading to photobleaching over a 1 h time scale. **a** FITC loaded HUVEC cells. **b** 30 nm fluorescent silica loaded cells. **c** 100 nm fluorescent silica loaded cells. The cells are incubated with 100 μg/ml of nanomaterials for 3 h and are washed and subjected to continued irradiation for a period of 1 h. Images are taken every 20 min and the photobleaching of pure FITC and FITC loaded nanomaterials are studied

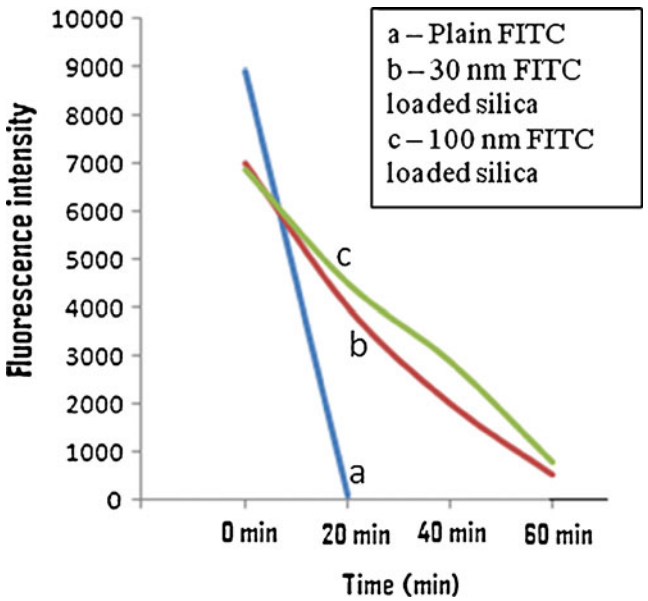

Fig. 13 Fluorescence intensity graph of fluorescent silica nanoparticles endocytosed in HUVEC cells under continued irradiation

silica nanoparticles provide higher photostability than the dye alone, making them suitable for imaging live cells. This high photostability can be attributed to the FITC being entrapped within the silica matrix. Thereby we propose that the photostability of the dye can be increased by silica layers and could be efficiently used in cell tagging. It was noted that even though the 30 nm FITC loaded silica particles were effectively functional till the 4th day, their intensity reduced substantially over a period of time. We hypothesize that this may be due to the less amount of FITC cargo loaded into the 30 nm particles compared to the 100 nm particles which is evidenced by the mass loss percentage observed with TGA.

Flow cytometry was carried out to investigate the co-localization of both DAPI signal and FITC doped nano silica signal in a single cell with 50 μg of FITC loaded silica particles. Flow cytometry cannot differentiate between particles attached to the cells and the internalized ones. So the cells were washed repeatedly and then stained with trypan blue which can neutralize the

fluorescence of nanomaterials attached outside the cell. Cells were viewed under confocal microscope for localized nanomaterials and then subjected to flow cytometry, fluorescence intensity graphs were obtained for DAPI and FITC signal using their appropriate filters (Fig. 14). Overlap of both the signals confirms the localization of DAPI and FITC in the same cells. This also proves the endocytosis of nanomaterials into live HUVEC cells. The intensity of DAPI staining noted in intensity plot was greatly appreciated because it directly correlates to the live cells.

Conclusion

To summarize, we demonstrated that endocytosis of dye loaded variable sized nanomaterials are possible in living cells. We have successfully reported the use of 30 nm nanosilica as efficient cell tags. These 30 nm and 100 nm particles show excellent biocompatibility and perfect endocytosis with the latter possessing higher efficacy. It was also proved that the nanomaterials escape the endosomes after a period of time projecting their potential application in drug delivery too. Compared to the free dye, the FITC loaded nanomaterial's photostability is increased, equally supplemented by reduced photobleaching under continued irradiation with fluorescence observed upto a week in case of no irradiation. Thus these fluorescent particles are proposed as highly efficient cell tags and can be directed for diagnostic targeting if surface functionalized. This study may allow us to visualize more accurate therapeutic delivery and diagnostic imaging based on silica nanomaterials in near future.

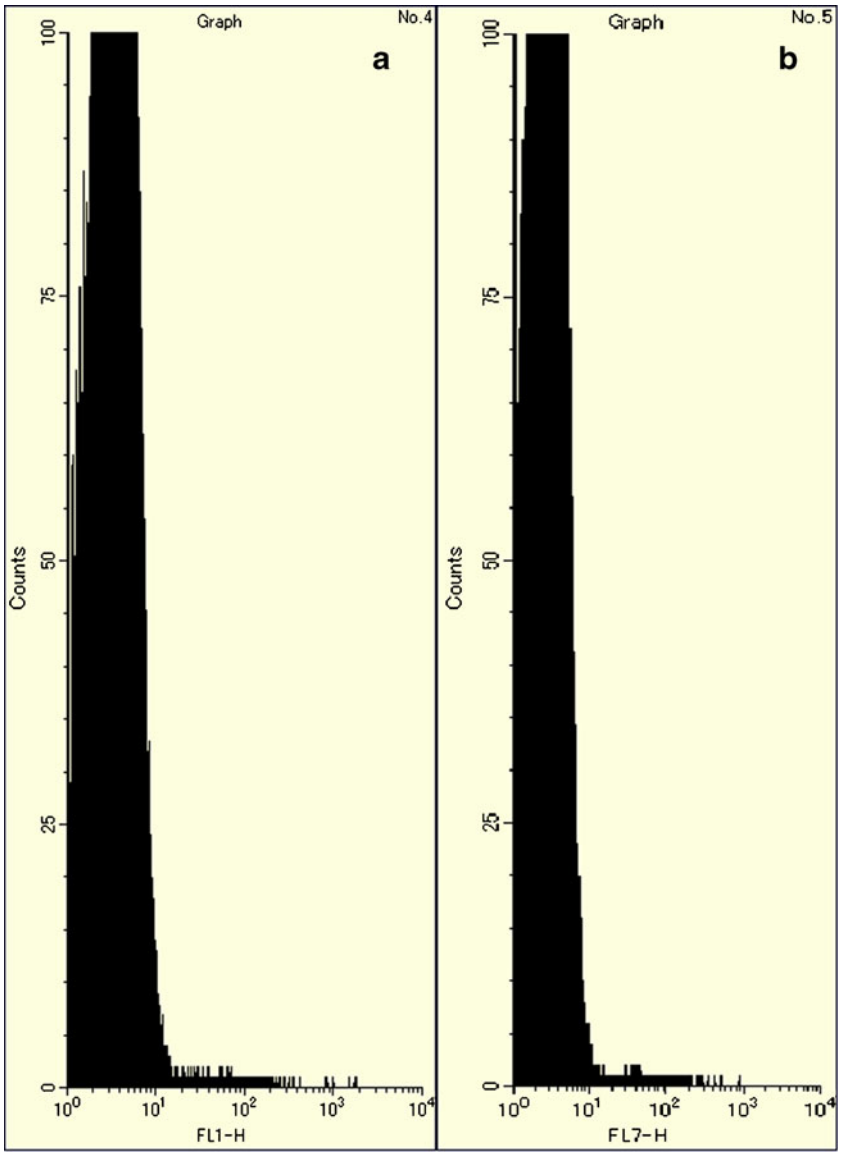

Fig. 14 Flow cytometry to study colocalization of FITC and DAPI signals. These two graphs shows colocalized **a** DAPI and **b** FITC staining. The cells are grown for 48 h and then incubated with nanomaterials and are trypsinized and fixed with ethanol after DAPI staining

Acknowledgement Srivani Veeranarayanan, Aby Cheruvathoor Poulose, Sheikh Mohamed and Athulya Aravind thank Ministry of Education, Culture, Sports, Science and Technology (MEXT), Japan for providing financial support, the Monbukagakusho fellowship. Authors thank Prof. Fukushima for Photoluminescence measurement and Dr. Iwai for guiding in Flow cytometry analysis.

References

1. Santra S, Liesenfeld B, Bertolino C, Dutta D, Cao Z, Tan W, Moudgil BM, Mericle RA (2006) Fluorescence lifetime measurements to determine the core–shell nanostructure of FITC-doped silica nanoparticles: an optical approach to evaluate nanoparticle photostability. J Lumin 117(1):75–82
2. Larson DR, Zipfel WR, Williams RM, Clark SW, Bruchez MP, Wise FW, Webb WW (2003) Water-soluble quantum dots for multiphoton fluorescence imaging in vivo. Science 300 (5624):1434–1436
3. Babes L, Denizot B, Tanguy G, Jeune JJL, Jallet P (1999) Synthesis of iron oxide nanoparticles used as MRI contrast agents: a parametric study. J Colloid Interf Sci 212(2):474–482
4. Rosenholm JM, Meinander A, Peuhu E, Niemi R, Eriksson JE, Sahlgren C, Linden M (2009) Targeting of porous hybrid silica nanoparticles to cancer cells. ACS Nano 3(1):197–206
5. Barreto JA, O'Malley W, Kubeil M, Graham B, Stephan H, Spiccia L (2011) Nanomaterials: applications in cancer imaging and therapy. Adv Mater 23(12):H18–H40
6. Wu H, Huo Q, Varnum S, Wang J, Liu G, Zimin N, Liu J, Lin Y (2008) Dye-doped silica nanoparticle labels/protein microarray for detection of protein biomarkers. Analyst 133(11):1550–1555
7. Bailey RE, Smith AM, Shuming N (2004) Quantum dots in biology and medicine. Phys E 25(1):1–12
8. Li KG, Chen JT, Bai SS, Wen X, Song SY, Yu Q, Li J, Wang YQ (2009) Intracellular oxidative stress and cadmium ions release induce cytotoxicity of unmodified cadmium sulfide quantum dots. Toxicol Vitr 23(6):1007–1013
9. Lin Y-S, Tsai C-P, Huang H-Y, Kuo C-T, Hung Y, Huang D-M, Chen Y-C, Mou C-Y (2005) Well ordered mesoporous silica nanoparticles as cell markers. Chem Mater 17(18):4570–4573
10. Santra S, Yang H, Dutta D, Stanley JT, Holloway PH, Tan W, Moudgil BM, Mericle RA (2004) TAT conjugated, FITC doped silica nanoparticles for bioimaging applications. Chem Commun (24):2810–2811
11. Mal NK, Fujiwara M, Tanaka Y (2003) Photocontrolled reversible release of guest molecules from coumarin-modified mesoporous silica. Nature 421(6921):350–353
12. He X, Duan J, Wang K, Tan W (2004) A novel fluorescent label based on organic dye-doped silica nanoparticles for HepG liver cancer cell recognition. J Nanosci Nanotech 4(6):585–589
13. Slowing II, Vivero-Escoto JL, C-W Wu, Lin VS-Y (2008) Mesoporous silica nanoparticles as controlled release drug delivery and gene transfection carriers. Adv Drug Delivery Rev 60(11):1278–1288
14. Liong M, Lu J, Kovochich M, Xia T, Ruehm SG, Nel AE, Tamanoi F, Zink JI (2008) Multifunctional inorganic nanoparticles for imaging, targeting, and drug delivery. ACS Nano 2(5):889–896
15. Nair R, Poulose AC, Nagaoka Y, Yoshida Y, Maekawa T, Kumar DS (2011) Uptake of FITC labeled silica nanoparticles and quantum dots by rice seedlings: effects on seed germination and their potential as biolabels for plants. J Fluoresc. doi:10.1007/s10895-011-0904-5
16. Lai CY, Trewyn BG, Jeftinija DM, Jeftinija K, Xu S, Jeftinija S, Lin VS-Y (2003) A mesoporous silica nanosphere-based carrier system with chemically removable CdS nanoparticle caps for stimuli-responsive controlled release of neurotransmitters and drug molecules. J Am Chem Soc 125(15):4451–4459
17. Lin Y-S, Hung Y, Su JK, Lee R, Chang C, Lin M-L, Mou C-Y (2004) Gadolinium(III)-incorporated nanosized mesoporous silica as potential magnetic resonance imaging contrast agents. J Phys Chem B 108(40):15608–15611
18. Trewyn BG, Nieweg JA, Zhao Y, Lin VY-S (2008) Biocompatible mesoporous silica nanoparticles with different morphologies for animal cell membrane penetration. Chem Eng J 137(1):23–29
19. Yang J, Lee J, Kang J, Lee K, Suh JS, Yoon HG, Huh YM, Haam S (2008) Hollow silica nanocontainers as drug delivery vehicles. Langmuir 24(7):3417–3421
20. Chen JF, Ding HM, Wang JX, Shao L (2004) Preparation and characterization of porous hollow silica nanoparticles for drug delivery application. Biomaterials 25(4):723–727
21. Vallhov H, Gabrielsson S, Strømme M, Scheynius A, Garcia-Bennett AE (2007) Mesoporous silica particles induce size dependent effects on human dendritic cells. Nano Lett 7 (12):3576–3582
22. Lu J, Liong M, Zink JI, Tamanoi F (2008) Mesoporous silica nanoparticles as a delivery system for hydrophobic anticancer drugs. Small 3(8):1341–1346
23. Rosenholm JM, Peuhu E, Eriksson JE, Sahlgren C, Linden M (2009) Targeted intracellular delivery of hydrophobic agents using mesoporous hybrid silica nanoparticles as carrier systems. Nano Lett 9(9):3308–3311
24. Suzuki K, Kenichi Ikari K, Imai H (2004) Synthesis of silica nanoparticles having a well-ordered mesostructure using a double surfactant system. J Am Chem Soc 126(2):462–463